

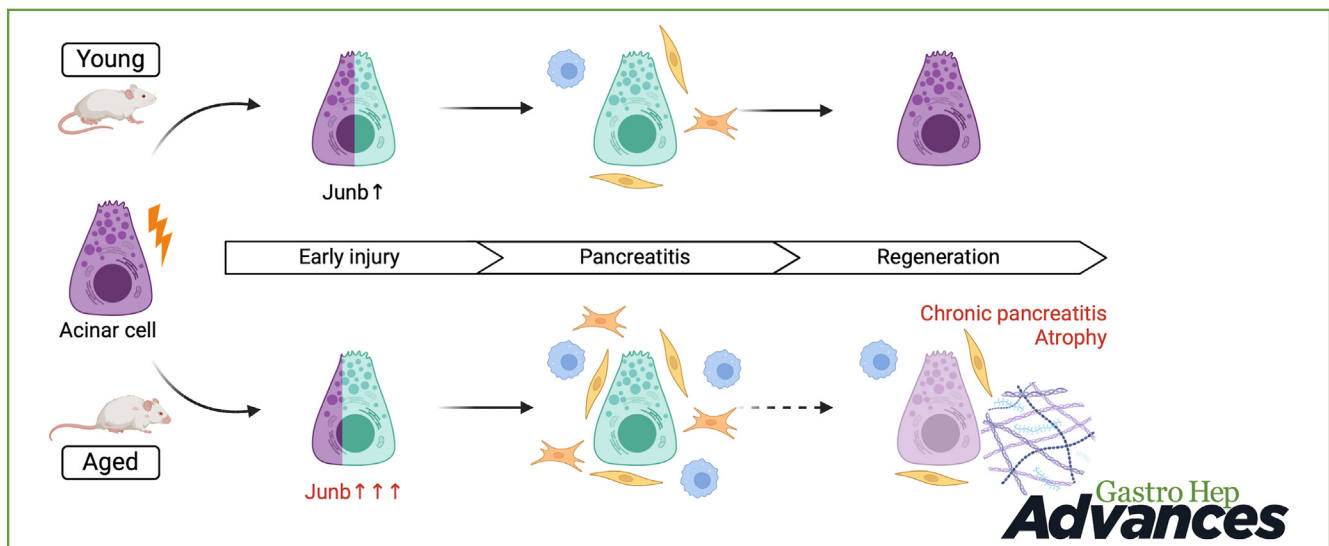
ORIGINAL RESEARCH—BASIC

Age-Related Decline in Pancreas Regeneration Is Associated With an Increased Proinflammatory Response to Injury



Kristina Høj,¹ Jonathan Baldan,^{1,†} Philip Allan Seymour,¹ Charlotte Vestrup Rift,² Jane Preuss Hasselby,² Albin Sandelin,^{1,3} and Luis Arnes¹

¹Biotech Research and Innovation Centre (BRIC), University of Copenhagen, Copenhagen, Denmark; ²Department of Pathology, Copenhagen University Hospital Rigshospitalet, Copenhagen, Denmark; and ³Department of Biology, University of Copenhagen Copenhagen, Denmark



BACKGROUND AND AIMS: The regenerative capacity of the pancreas diminishes with age. Understanding acinar cell responses to injury and the resolution of regenerative processes is crucial for tissue homeostasis. However, knowledge about the impact of aging on these processes remains limited. **METHODS:** To investigate the influence of aging on pancreas regeneration, we established a cohort of young (7–14 weeks) and old (18 months) C57bl/6 mice. Experimental pancreatitis was induced using caerulein, and pancreas samples were collected at various time points after induction, covering acute damage response, inflammation, peak proliferation, and inflammation resolution. Our analysis involved immunohistochemistry, quantitative imaging, and gene expression analyses. **RESULTS:** Our study revealed a significant decline in the regenerative capacity of the pancreas in old mice. Despite similar morphology and transcriptional profiles between the pancreas of young and old mice under homeostasis, the aged pancreas is primed to generate an exacerbated proinflammatory reaction in response to injury. Specifically, we observed notable upregulation of *Junb* expression in acinar cells and aberrant myofibroblast activation in the aged pancreas. **CONCLUSION:** The response of acinar cells to injury in the pancreas of aged mice is characterized by an increased susceptibility to inflammation and stromal reactions. Our findings uncover a pre-existing proinflammatory state in aged acinar cells, offering insights into potential strategies to prevent the onset of pancreatic insufficiency and the development of inflammatory conditions.

These insights hold implications for preventing conditions such as chronic pancreatitis and pancreatic ductal adenocarcinoma.

Keywords: ADM; Plasticity; Aging; Junb

Introduction

Acute pancreatitis is one of the most prevalent gastrointestinal causes for hospitalization, with its global incidence steadily increasing.¹ In contrast to the

[†]Current address: Translational Oncology Research Center, Vrije Universiteit Brussel (VUB), Brussels, Belgium.

Abbreviations used in this paper: ADM, acinar-to-ductal metaplasia; AP, activator protein; CAE, caerulein; DAB, 3,3'-diaminobenzidine tetra hydrochloride; FGSR, Fast Green and Sirius Red; GSEA, gene set enrichment analysis; IL, interleukin; KRAS, Kirsten rat sarcoma proto-oncogene; MFI, mean fluorescence intensity; PBS, phosphate-buffered saline; PDAC, pancreatic ductal adenocarcinoma.

Most current article

Copyright © 2024 The Authors. Published by Elsevier Inc. on behalf of the AGA Institute. This is an open access article under the CC BY-NC-ND license (<http://creativecommons.org/licenses/by-nc-nd/4.0/>).

2772-5723

<https://doi.org/10.1016/j.gastha.2024.07.002>

young population, elderly individuals frequently manifest severe acute pancreatitis.² The clinical trajectory in this age group tends to be less predictable, leading to more adverse outcomes that often culminate in multi-organ failure and elevated mortality rates.²⁻⁴ Aging impacts the homeostatic mechanisms necessary for tissue function and regeneration.⁵ Notably, the pancreas of older individuals displays morphological alterations, associated with increased systemic inflammation and thrombosis, including atrophy, fibrosis, and lymphocyte infiltration.^{6,7} While our understanding of tissue homeostasis and adaptation to injury in the pancreas is expanding, the effects of aging on these processes remain less understood.

Pancreatic injury triggers acinar cells within the exocrine tissue to undergo acinar-to-ductal metaplasia (ADM), a complex process involving the cessation of their dedicated secretory program and the acquisition of traits similar to ductal cells and embryonic progenitors.^{8,9} ADM provides acinar cells the ability to re-enter the cell cycle while simultaneously coordinating tissue remodeling by attracting immune cells, activating fibroblasts, and inducing modifications in the extracellular matrix to facilitate efficient tissue repair.¹⁰ The maladaptation of acinar cells to injury or the failure to resolve the regenerative response results in an exacerbated activation of fibroblasts, deviations in the composition of infiltrating immune cells, fibrosis, and ultimately a decline in tissue regeneration and loss of function.¹¹⁻¹³ The activator protein (AP)-1 family of transcription factors regulates the transcriptional shift in acinar cells, transitioning them from their differentiated secretory function to a proinflammatory response.¹⁴ This shift plays a crucial role in regulating the activation of resident tissue fibroblasts and the recruitment of immune cells to the injury site, thereby fostering an environment conducive to tissue repair.¹⁵ Furthermore, activating mutations in the Kirsten rat sarcoma proto-oncogene (KRAS) impede the resolution of the regenerative process, leading to an irreversible state of acinar injury.¹⁶ This process is mediated by the irreversible deposition of *Junb*, a member of the AP-1 family of transcription factors, at regulatory elements of ADM drivers and inflammatory cytokines. Similarly, analysis of chromatin accessibility in sorted acinar cells has identified newly accessible chromatin domains in proinflammatory cytokines during the progression from homeostasis to ADM to KRAS-induced neoplastic transformation.¹⁷ It is important to note that the molecular analysis of chronic pancreatitis and early neoplastic lesions demonstrates that they share molecular signatures and cellular composition.¹⁷⁻²⁰ These studies highlight a progressive dysregulation of acinar adaptation to injury, a proinflammatory regulatory network, and an exacerbated response of the tissue microenvironment as determinants of disease severity. Overall, although we are gaining extensive knowledge in the mechanisms regulating tissue homeostasis in the pancreas, the effect of aging on acinar adaptation to injury and the capacity to resolve the regenerative program remains to be elucidated in old individuals.

Materials and Methods

In Vivo Mouse Experiments

Young (7–14 weeks of age) and aged (18 months of age) C57Bl/6J mice were administered with various bouts of caerulein (CAE) (Sigma-Aldrich #C9026). Acute pancreatitis was induced by 8 hourly intraperitoneal injections of CAE (125 µg/kg per injection) on 2 consecutive days, and mice were sacrificed immediately after the last injection (D0), 2 days (D2), or 14 days later (D14). To investigate the early damage response, mice were sacrificed after four-hourly injections (5H). Control mice were non-injected or injected with phosphate-buffered saline (PBS). Animals were housed in accordance with the best animal husbandry guideline recommendations of the European Union Directive (2010/63/EU). The Danish Animal Experiments Inspectorate reviewed and approved all animal experiments.

Immunohistochemistry and Immunofluorescence

Pancreata were fixed in 4% paraformaldehyde (VWR Chemicals # 9713-1000) for 24 hours (for paraffin) or 3 hours (for O.C.T.) and subsequently dehydrated in 70% ethanol (VWR Chemicals # 20824.365) at room temperature until paraffin embedding or 30% sucrose for cryoprotection in O.C.T.

Tissues were cut into 4 µm representing different depths of the tissue sections and placed on Superfrost Plus slide (10149870; Fisher Scientific). Antigen retrieval was performed in Tris-ethylenediaminetetraacetic acid buffer (pH 9). Sections were washed in PBS-Tween 0.5% and blocked with 1% donkey serum before incubation with primary antibodies overnight at 4 degrees. Secondary antibodies + 4',6-diamidino-2-phenylindole were incubated for 1 hour at room temperature. Sections were mounted with Vectashield Mounting medium (H-1000; Vector Laboratories). Images were acquired using ScanR (Olympus) or a confocal microscope (Leica SP8) using the same laser intensities and parameters.

For immunohistochemistry, after overnight incubation with the primary antibody, the sections were washed in PBST and endogenous peroxidase activity was suppressed using Peroxidase Suppressor (Thermo Scientific # 35000). This was followed by incubation with the relevant horseradish peroxidase-conjugated secondary antibody for 1 hour and a 15-minute incubation with Metal enhanced 3,3'-diaminobenzidine tetra hydrochloride (DAB) substrate working buffer (Metal Enhanced DAB Substrate Kit, Thermo Scientific, USA). Slides were counterstained with hematoxylin (3 min) and blueing agent (H&E Staining Kit, Abcam # ab245880). Finally, the sections were dehydrated in 100% ethanol (1 minute) and xylene (1 minute) before mounting with Entellan (Sigma-Aldrich, Germany # 107960) with coverslips (Thermo Scientific #15747592). Whole section imaging was acquired using NanoZoomer-XR Digital slide scanner C12000-01 (Hamamatsu). For antibodies applied, see [Table A1](#).

For Fast Green and Sirius Red (FGSR) stain, sections were deparaffinized in xylene and rehydrated through 100%, 70%, and 50% ethanol to water. Sections were covered with 0.1% Fast Green (Sigma #F7258) and 0.1% Sirius Red (Sigma #365548) in saturated picric acid solution (Merck #P6744) and incubated for 1 hour at room temperature. The sections were dehydrated in 100% ethanol, cleared in xylene before mounting with Entellan (Sigma-Aldrich, Germany # 107960). Whole section imaging was acquired using NanoZoomer-XR Digital slide scanner C12000-01 (Hamamatsu).

Image Processing

For quantification of acinar and tissue area in H&E-stained sections, QuPath (open-source software for bioimage analysis) was applied. The polygon tool was used to loosely define the area of interest, that is, excluding spleen and artefacts. The threshold settings were adapted accordingly and saved as a classifier to be applied across all images. Similarly, a threshold was created within the tissue annotation to measure the acinar area with parameters adjusted for eosin stain. Non-acinar regions such as ducts, veins, and arteries were manually removed. Similar to H&E quantification, quantification of FGSR stain was done using QuPath Pixel Thresholder. A tissue annotation was created based on the threshold for average channels, including interlobular spaces clearly within the tissue area while excluding spleen and artefacts. Within the tissue annotation, an annotation was created based on the Sirius Red Pixel threshold, yielding area measurements of both annotations. For F4/80 quantification, a tissue annotation was defined as for FGSR. However, F4/80 positive cells within this annotation were quantified using Positive Cell Detection based on an appropriate threshold for “DAB optical density mean” intensity. Similarly, cleaved caspase 3 quantification was done using Positive Cell Detection within a stricter Pixel threshold-created tissue annotation to restrict the detection of positive nuclei to being within pancreatic lobules.

Cell detection, classification, and intensity measurement of immunofluorescence using QuPath. Quantification of Vimentin (Vim⁺), alpha-smooth muscle actin (α SMA⁺), Junb⁺, Ecad⁺ cells were based on up to 25 images per section, obtained from ScanR microscope, and quantified using QuPath. Two sections were analyzed per tissue. *Cell detection* was adjusted to the 4',6-diamidino-2-phenylindole intensity and applied to all images with the same parameters. *Cell classification* was trained in a random image. The “Points” tool was used to manually annotate a number of cells positive for a given channel, and the *Train object classifier* was used for automatic annotation. The training was repeated in other channels when needed. The single classifier or merged multiple classifiers were run for each image yielding a total number of detections and the number of classified detections for each channel per image. Junb intensity was measured in QuPath using the Set cell intensity classification tool on top of already run Cell Detection and Object Classification. Here pixel value thresholds (arbitrary units) of “Nucleus: Junb mean” were set as follows: low (<1500), medium (1500–2500), and high (>2500). This yielded the number of Ecad-positive cells falling within each of the Junb mean intensity ranges. The threshold for “low” was set based on control tissues (young and aged) to exclude background staining.

Intensity measurement using ImageJ. To measure Mist1 intensity, Mist1 channel images acquired from a confocal microscope were opened in ImageJ. The threshold was set automatically on a random image of the 5H time point since this was expected to be lower in intensity. This threshold was applied to all images for quantification. For background normalization, a rectangle was drawn in the background of each image, and the mean fluorescence intensity (MFI) within the rectangle was measured. Then the background MFI was subtracted from the MFI of the region of interest, yielding the final MFI value.

Gene Expression Analyses

RNA was extracted using the RNeasy Mini Kit following manufacturer instructions (Qiagen #74106). DNA removal was performed with the DNase I Amplification Grade kit (Thermo Fisher Scientific, USA) and stored at -20°C . Expression levels were calculated using the comparative ddCT method of relative quantitation, with *ribosomal protein L5 (Rpl5)* and *ribosomal protein S2 (Rps29)* as housekeeping genes. For primer sequences, see Table A1.

RNA-sequencing and downstream analyses. Bulk RNA from control and 5H time points of young and aged mice were sequenced in Illumina NovaSeq 6000 Sequencing System with paired-end 150 bp read length and output of ≥ 20 million read pairs per sample (Novogene). Bioinformatic analysis provided by Novogene unless otherwise indicated. Visualization of differentially expressed genes by volcano plot was done in R Studio (v2023.06.1 + 524) using the packages; tidyverse, ggplot, and ggrepel. Gene set enrichment analysis (GSEA) was performed on count data derived from RNA-seq data against Hallmark signatures in the MSigDB database (GSEA v4.3.2, Broad Institute). The default settings were used except for *collapse to gene symbols* and *permutation type: gene_set*. For all analyses, the *metric for ranking genes* was *Signal2Noise* except for the comparisons including A_control where *Diff_of_Classes* was used. This was due to an $n = 2$ which was not applicable for *Signal2Noise*.

Motif analysis. HOMER was used to do motif analysis with a standard setting.²¹ We tested either up-regulated genes ($\log_2\text{FC} > 0.5$ and $\text{FDR} < 0.05$) or downregulated genes ($\log_2\text{FC} < 0.5$ and $\text{FDR} < 0.05$) vs a background of non-changing genes ($-0.5 > \log_2\text{FC} > 0.5$, $\text{FDR} > 0.05$), based on the DESeq2 analysis from Table A2. For each gene ID in each such gene set, HOMERs in-built sequence feature retrieval function was used to identify the -1000 to $+100$ region around the ENSEMBL-annotated TSS (mm 10 assembly). Only known motif overrepresentation was reported in this analysis.

Statistical Analyses

Plots and statistical analyses were done using GraphPad Prism (v.9.5.1). For quantitative polymerase chain reaction, the statistical significance of differences between 2 experimental groups was assessed by one-way analysis of variance (P value $< .05$). For multiple conditions, one-way analysis of variance was used with correction for multiple comparisons using Tukey (P value $< .05$). The significance of gene sets from GSEA was based on a nominal P value $< .05$ and an FDR q -value < 0.25 .

Pancreas regeneration is compromised in old mice. In this study, we aimed to discern the impact of aging on the adaptive behavior of pancreatic acinar cells and the regenerative potential of the pancreas following acute pancreatitis. To achieve this objective, we employed a mouse model of pancreatic injury through repeated administration of supra-physiological levels of a cholecystokinin analogue, CAE.^{8,22} This model was applied to both young (7–14 weeks) and old (18 months) C57Bl/6 mice (Figure 1A). Histological examinations of the pancreas in both young and old mice revealed normal morphology, characterized by overall normal architecture, well-defined lobules, and the absence of discernible immune

infiltration within the interlobular space. The acinar cells displayed their characteristic pyramidal shape, and the ducts exhibited a single layer of cuboidal epithelial cells (Figure 1B). In the group subjected to CAE-induced injury, we observed evident significant alterations in pancreatic morphology. Both young and old mice displayed signs of acute inflammation with granulocytes and lymphocytes. Oedematous acini, focally dilated and enlarged intralobular space, obvious immune infiltration, and acinar to ductal metaplasia, indicative of inflammatory tissue response (Figure 1B). Remarkably, while the young mice demonstrated complete recovery within a 14-day period, the old mice displayed notable pancreatic atrophy and morphological signs of chronic inflammation with fibrosis around ducts and infiltration of lymphocytes (Figure 1B). We quantified this observation by whole-slide imaging through quantification of acinar area relative to tissue area, which highlighted a substantial reduction in acinar tissue in old mice when comparing the 2 age groups (Figure 1C). This ratio is based on measurements of eosin-dense areas, where a decrease indicates a loss of the protein-rich acinar cell phenotype. Moreover, pathological evaluation by expert pathologists who were blinded to the experimental groups revealed significant differences: all 4 pancreases from the old mice exhibited

atrophy, loss of acini, and focal loss of lobular architecture, in contrast to only one of the 3 young mice, where the damage was more localized (Table A3 and Figure A1). Collectively, while the aged pancreas exhibited comparable tissue morphology and responses to tissue damage as observed in the young pancreas, the regenerative capability was significantly impaired in the older mice by day 14. These findings underscore a marked diminishment in pancreas recovery following experimental pancreatitis with the progression of age.

Acinar cells retain the proliferative capacity in old mice. Next, we sought to determine whether acinar proliferation and apoptosis were altered during pancreas regeneration in both young and old mice. We examined the proliferation index of epithelial and non-epithelial cells by immunofluorescence. Under basal conditions, the pancreas was mostly quiescent in young mice (Figure 2A), as expected.²³ Following the cessation of CAE treatment, the number of proliferating epithelial cells (marked by Ki67+) increased in both young and old mice, precisely 2 days post treatment (Figure 2A and B). Interestingly, in the context of aged mice, we did not observe any discernible differences compared to the young (Figure 2A and B). Moreover, although acinar cell

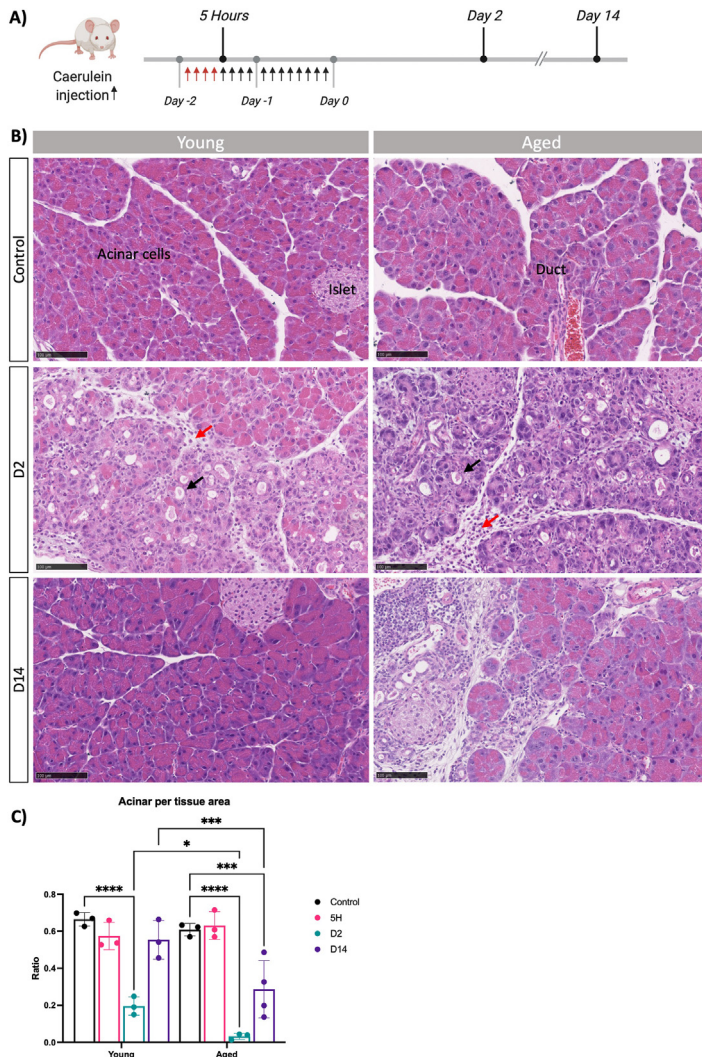
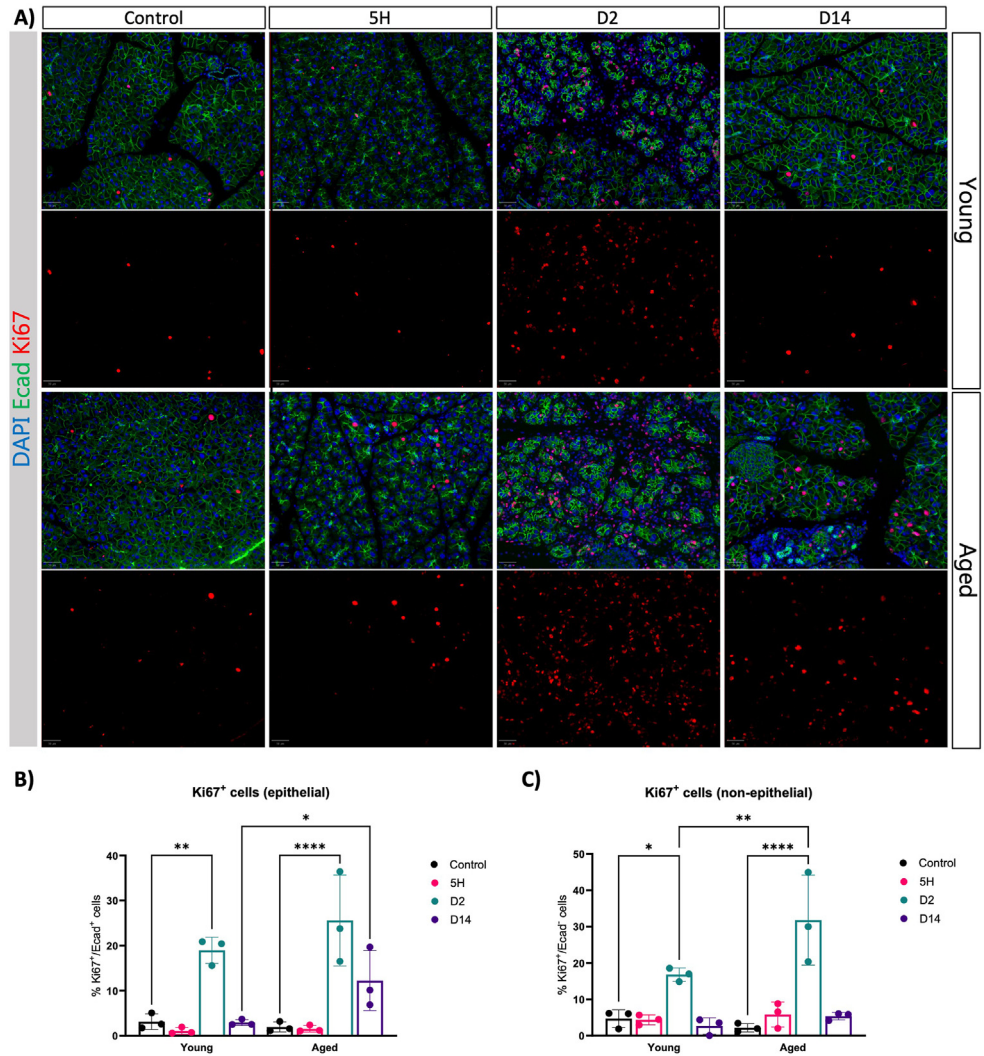


Figure 1. Pancreas regeneration is affected with aging. (A) Schematic representation of the experimental model to induce acute pancreatitis in young and old mice. (B) Representative H&E images of indicated conditions of young (left) and aged (right) mouse pancreas. Scale bars represent 100 μm. Arrows indicate infiltration (red) and apparent ADMs (black). (C) Quantification of ratio acinar area per tissue area in young and aged mice. At least 3 mice per group. Statistical analysis was determined by two-way analysis of variance. Error bars represent SD. Values of significance: ns $P > .05$ is omitted, $*P \leq .05$, $***P \leq .001$, $****P \leq .0001$.

Figure 2. Aging does not affect the capacity of acinar cells to enter the cell cycle. (A) Immunofluorescence of Ecad and Ki67 at given time points after caerulein treatment in young and aged mice. DAPI was used as a counterstain to visualize nuclei. Images were acquired using ScanR, and representative images were shown ($n = 3$). Scale bars represent $50 \mu\text{m}$. (B) Percentage of epithelial cells (Ecad+) that are proliferating (Ki67+). (C) Percentage of non-epithelial cells (Ecad-) that are proliferating (Ki67+). Statistical analysis was determined by two-way analysis of variance. Error bars represent SD. Values of significance: ns $P > .05$ is omitted, * $P \leq .05$, ** $P \leq .01$, *** $P \leq .001$, **** $P \leq .0001$. DAPI, 4',6-diamidino-2-phenylindole.



proliferation reverted to basal levels 14 days after injury in the young, the residual acinar cell population within the elderly mice demonstrated a sustained capacity for initiating proliferation (Figure 2B). Hence, the impaired regenerative capacity in the aged pancreas cannot be attributed to a defect in acinar proliferation. We detected an increase in cleaved caspase 3 positive cells on day 2 that was marginally, yet significantly, higher in older mice (Figure A2). Our observations also unveiled an elevated number of proliferating cells within the non-epithelial compartment, exclusively at day 2, across both age groups (Figure 2C). The proportion of Ki67+ cells was higher in old mice compared to young individuals. These findings suggest that the increased proliferation among non-epithelial cells may be indicative of an exaggerated stromal reaction in aged mice compared to young individuals.

Old mice showed an increased proinflammatory response upon tissue injury. To obtain a more precise understanding of the acinar adaptation to injury in old and young mice, we performed Junb immunofluorescence analysis. We observed Junb upregulation as early as 5 hours of initiating the CAE injections, which was maintained after 2 days of the last CAE injection in young and old mice (Figure 3A). We observed an increase in the number of Junb +

cells predominantly of epithelial origin in old mice (Figure 3B) and an increased intensity of Junb staining per cell (Figure 3C). Notably, at the early stages of tissue injury, the pancreas showed a normal histology with no evidence of immune infiltration or fibroblast activation (Figure A3A). We did not observe Junb upregulation in islets or ductal cells (Figure A3B). Indicating that Junb expression following CAE injury is restricted to the acinar cells. Despite regeneration being severely compromised in old mice, the expression of Junb returned to basal conditions in both age groups. Overall, our data suggest that the dynamics of Junb expression in acinar cells is similar in young and old mice. Indicating that acinar cells respond to the injury and can exit the regenerative program in young and old mice. However, acinar cells have an exacerbated response to tissue injury in old mice.

Acinar plasticity precedes tissue remodeling. Our data indicate that acinar response to injury is independent of changes in the morphology and cellular composition of the pancreas. This suggests that aging affects cell-autonomous processes in the acinar cells that contribute to the diminished regenerative capacity of the pancreas in old mice. In order to explore whether the acinar response to tissue injury during the early phases is cell autonomous, we conducted a

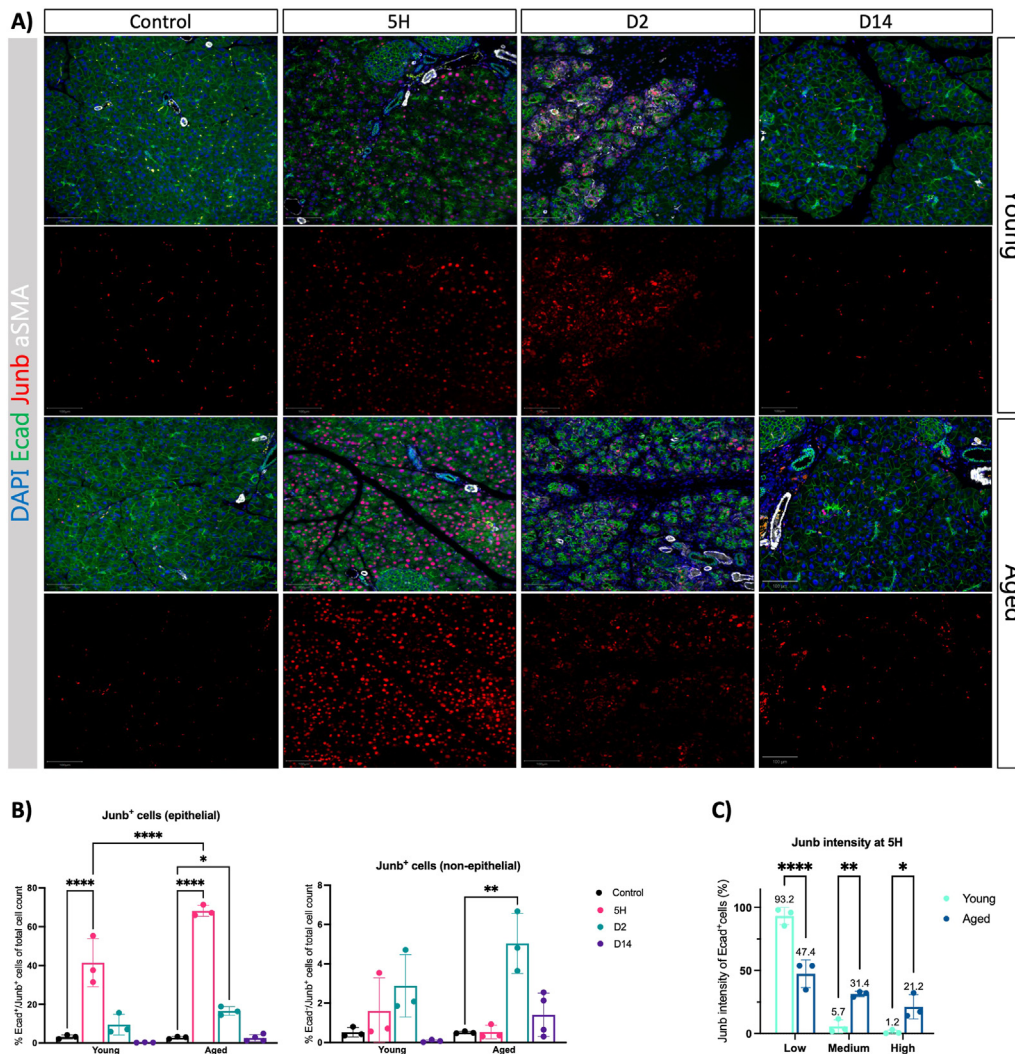


Figure 3. Junb expression is increased with aging. (A) Immunofluorescence of Ecad, Junb, and aSMA at given time points after caerulein treatment in young and aged mice. DAPI was used as a counterstain to visualize nuclei. Images were acquired using ScanR, and representative images were shown (n = 3). Scale bars represent 100 μm. (B) We quantified Junb + cells in the epithelial (Ecad+) and non-epithelial (Ecad-) compartments as a percentage of total cells in young and old mice at the time points indicated. (C) We quantified the number of epithelial (Ecad+) Junb + cells according to the immunofluorescent intensity of Junb in the 5-hour time point. Statistical analysis was determined by two-way analysis of variance. Error bars represent SD. Values of significance: ns $P > .05$ is omitted, * $P \leq .05$, ** $P \leq .01$, **** $P \leq .0001$. DAPI, 4',6-diamidino-2-phenylindole.

comprehensive time course experiment employing both quantitative polymerase chain reaction and histopathological analysis. First, we focused on young mice to avoid confounding effects associated with aging. Our findings revealed a swift increase in Sox9 expression, a marker of ADM, emerging as early as 2 hours after CAE injection (Figure A4A). In addition to the upregulation of ductal markers, acinar adaptation to injury is associated with the upregulation of pancreas progenitor markers and the concomitant downregulation of the master regulator of the acinar program.^{8,24} We observed upregulation of Krt19 and Notch signaling (Hes1 transcription factor) as early as 2 hours after CAE injection (Figure A4A). Furthermore, while the abundance of Mist1+ cells, the master regulator of acinar differentiation (also called Bhlha15), remained unchanged at the 5-hour mark (Figure A4B), Mist1 expression was significantly downregulated (Figure A4C). To assess potential

alterations in Mist1 protein expression during the initial response to damage, we acquired confocal microscopy images under uniform laser intensities (Figure A4D). Our observations show a decrease in Mist1 protein per cell at the 5-hour interval, indicating an ongoing process of acinar dedifferentiation at this stage. Cumulatively, our data indicate that acinar dedifferentiation and plasticity begin early in the process of tissue adaptation to the injury.

Aging is associated with an exacerbated activation of myofibroblasts. Next, we investigated the dynamics of acinar dedifferentiation and tissue remodeling in young and old mice during pancreas regeneration. We assessed the expression of *Vim*, *Acta2*, which encodes α SMA—a marker of activated fibroblasts—as well as macrophage-expressed gene (*Mpeg1*), protein tyrosine phosphatase

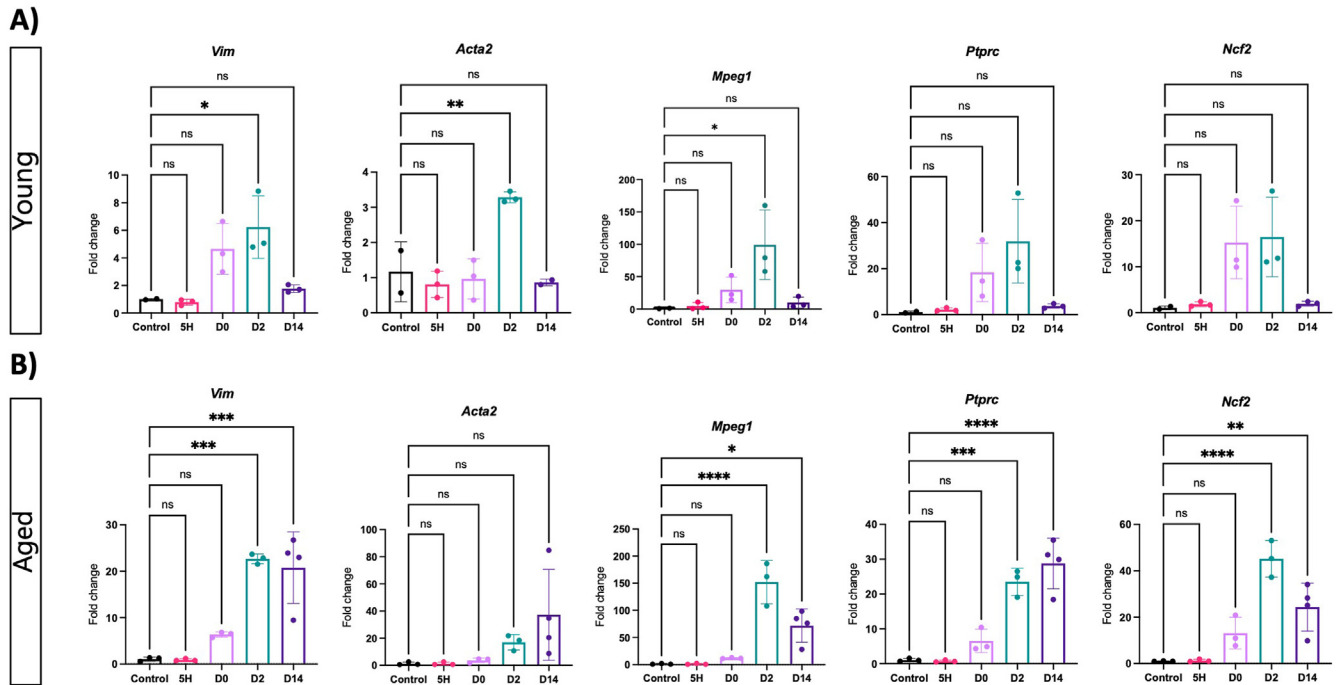


Figure 4. Aging exacerbates the remodeling of the tissue microenvironment in acute pancreatitis. Quantitative real-time polymerase chain reaction of microenvironment markers at given time points following caerulein treatment in young (A) and aged (B) mice. Fibroblast and fibroblast activation was determined by *Vim* and *Acta2* expression, respectively. Expression of immune cell markers was determined: *Mpeg1* for macrophages, *Ptprc* for leukocytes and *Ncf2* for neutrophils. Fold changes are shown relative to control and normalized with the housekeeping genes *Rpl5* and *Rps29*. Statistical analysis was determined by unpaired one-way analysis of variance. $n = 3$ mice per group, except $n = 2$ for young controls and young D14 for *Acta2* and $n = 4$ for aged D14. Error bars represent SD. Values of significance: $P > .05$ is ns, $*P \leq .05$, $**P \leq .01$, $***P \leq .001$, $****P \leq .0001$.

(*Ptprc*), and neutrophil cytosolic factor 2 (*Ncf2*), which are markers for macrophages, leukocytes, and neutrophils, respectively, and general indicators of myeloid cells. In young mice, an upregulation of α SMA and *Mpeg1* was observed, indicative of fibroblast activation and macrophage infiltration on day 2 following CAE treatment (Figure 4A). The values reverted to basal levels on day 14, in conjunction with the resolution of tissue injury. No discernible gene expression changes were observed between the control and the 5-hour time point, indicating that acinar dedifferentiation predates the activation of pancreatic fibroblasts and the infiltration of immune cells.

Subsequently, we assessed the dynamics of gene expression in the cohort of aged mice. Similar to young mice, the early phase of acinar dedifferentiation occurred independently of changes in the expression of tissue remodeling markers in old mice (Figure 4B). However, we noted an exacerbated increase in markers associated with activated fibroblasts and immune infiltration on day 2, an increased response that persisted even 14 days after CAE treatment, indicating a compromised acinar regeneration within the context of aging.

To support our observations, we conducted immunofluorescence analysis for *Vim* and α SMA in both young and aged mice. In alignment with the gene expression data, an increased number of *Vim* + cells and activated fibroblasts emerged on the second day within both age groups, especially enriched around presumed ADM lesions (Figure 5A). Interestingly, the proportion of α SMA + cells was notably higher in the older group

(Figure 5B). Supporting these findings, we observed an increase in the deposition of collagens as determined by FGSR staining (Figure A5). Next, we performed immunohistochemistry for F4/80 to assess macrophages presence in old and young mice. We observed an increased presence of macrophages in the pancreas on days 0 and 2 in young mice, with higher levels persisting in old mice even 14 days after injury induction (Figure A6). Our data suggest that the dynamics of tissue remodeling are similar in young and adult mice. Like young mice, the pancreas from old mice retained the capacity to acquire alternative cellular states in response to injury. However, the old mice exhibit an exaggerated response to injury, leading to an amplified activation of myofibroblasts, deposition of collagen, and infiltration of macrophages. Furthermore, the pancreas remains in a state of injury even 14 days after the cessation of CAE treatment.

Transcriptome analysis identify *Junb* dysregulation in old mice. To analyze the effects of aging and pancreatic injury at the transcriptional level, we performed RNAseq on the pancreata of young (7 weeks) and old (18 months) mice, both in homeostasis and 5 hours after CAE administration. Principal component analysis revealed that 67% of the variance among all groups could be explained by the administration of CAE, causing groups to cluster according to treatment conditions (Figure A7A). This infers that the transcriptional regulation of acinar cell function remains remarkably robust and is maintained in old mice. These results are

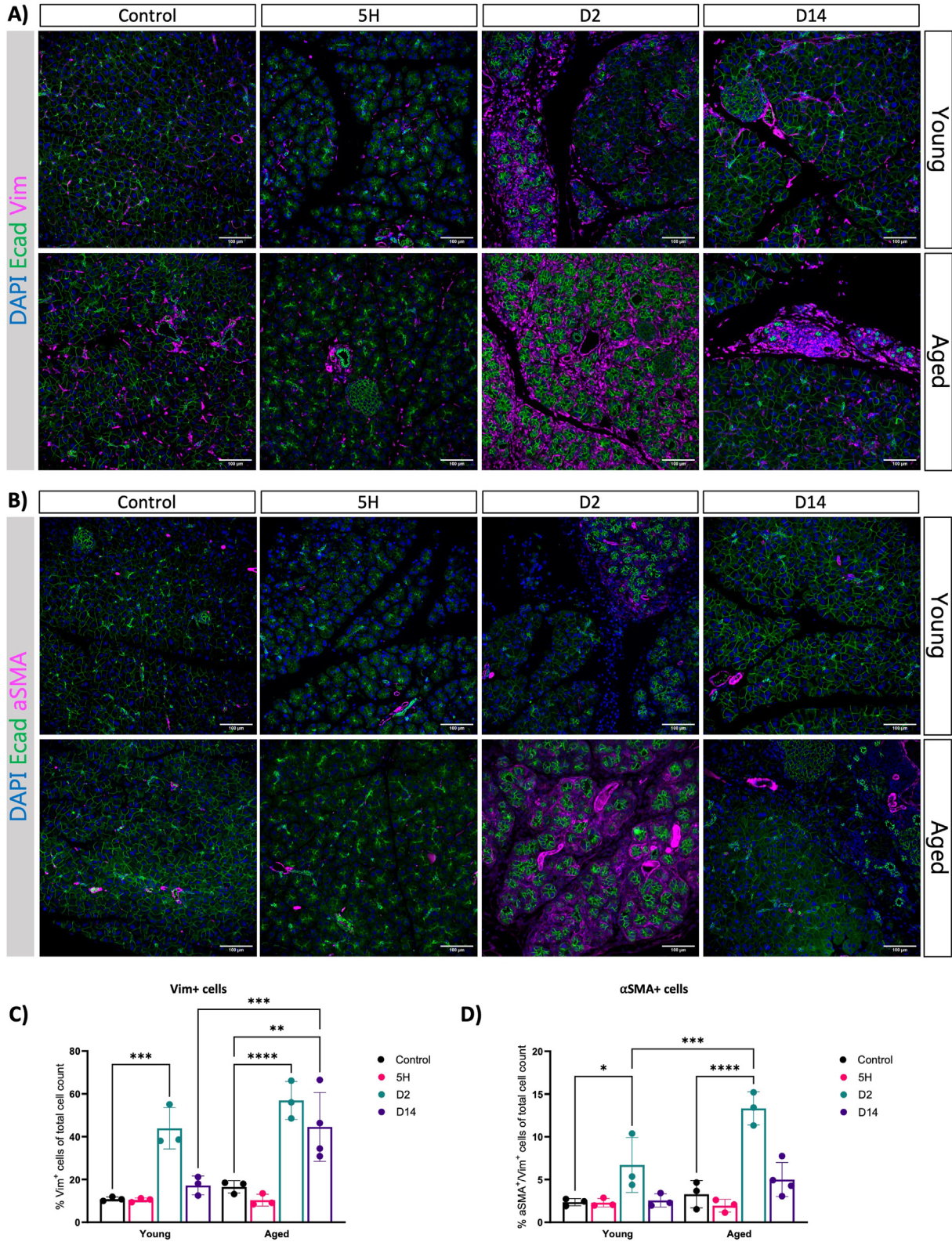


Figure 5. Fibroblast activation is increased in response to injury in old mice. (A and B) Immunofluorescence of Ecad and Vim (A) and Ecad and αSMA (B) at given time points after caerulein treatment in young and aged mice. DAPI was used as a nuclear counterstain. Images were acquired using ScanR, and scale bars represent 50 μm. (C and D) Quantification of IF showing the percentage of Vim⁺ (C) and Vim⁺αSMA⁺ (D) of total cell count. Statistical analysis was determined by two-way analysis of variance. At least 3 mice per group. Error bars represent SD. Values of significance: *P* > .05 is omitted, **P* ≤ .05, ***P* ≤ .01, ****P* ≤ .001, *****P* ≤ .0001. DAPI, 4',6-diamidino-2-phenylindole.

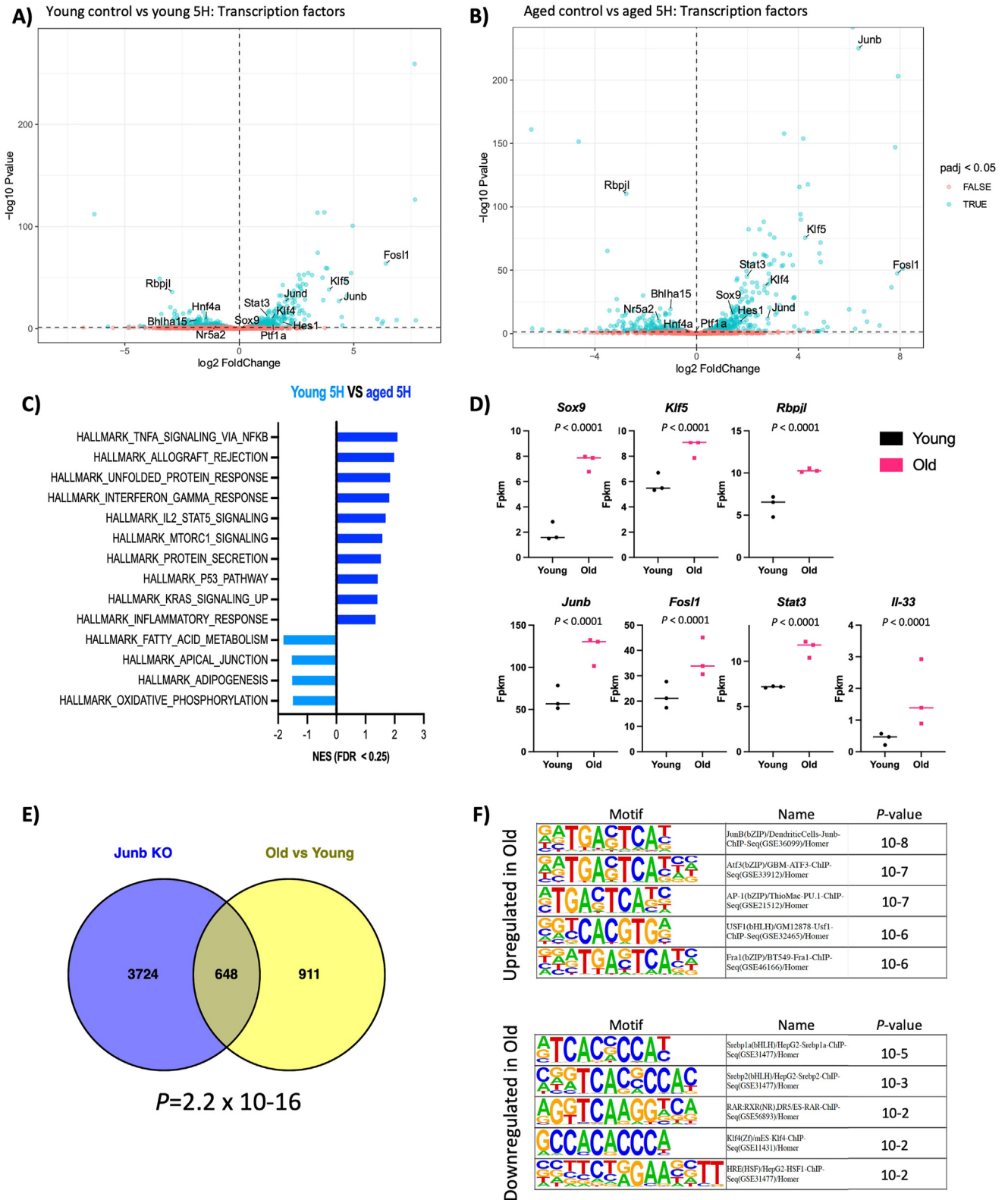


Figure 6. Acinar cells show a proinflammatory response to injury in aged mice. (A and B) Volcano plots showing statistical significance ($-\log_{10} P$ value) on the y-axis versus magnitude of fold change (\log_2 FC) on the x-axis. Each dot represents a gene. The genes are color-coded by adjusted P value ($padj$) < 0.05 (blue) and > 0.05 (red). (C) Gene set enrichment analysis of hallmark signature gene sets between 5H old and young mice. Significantly enriched hallmark signature gene sets were determined by FDR q -value < 0.25 and nominal P value $< .05$. (D) Differential gene expression analysis of selected genes as determined by RNAseq and DESeq2 analysis comparing old and young mice at the 5H time point. We observed upregulation of markers of pancreas development and proinflammatory signals in old mice compared to young. $n = 3$ mice/group. (E) Venn diagram

consistent with our previous histological analysis of the pancreas in both young and old mice.

Next, we conducted a differential gene expression analysis between age groups in the homeostatic state and identified a list of significantly differentially expressed genes ($n = 34$, $\text{padj} < 0.05$) (Table A4). Gene ontology analysis indicated increased lipid metabolism and decreased collagen deposition in the old group (Figure A7B).²⁵ Moreover, among the top downregulated and upregulated genes in the older pancreas were members of the regenerative (REG) protein family (*Reg3a*, *Reg2*, and *Reg3b*) and ribosomal proteins transcripts (*Rpl21*, *Rpl36*), respectively (Table A4). This finding aligns with the recently identified populations of regenerative (Acinar-REG+) and secretory acinar cells (Acinar-S).²⁰

To investigate the different responses to injury, we analyzed the effects of CAE treatment and identified many genes differentially expressed upon treatment in young and old mice ($n = 6060$ -young, $n = 6642$ -old, $\text{padj} < 0.05$) (Figure 6A and B; Tables A5 and A6). Despite the limited morphological alterations at this early time point, these results suggest that the pancreas has initiated an extensive transcriptional reprogramming in response to injury. As anticipated, GSEA analysis revealed enrichment of pathways associated with pancreatic injury (Figure A7C and D). We observed the upregulation of genes linked to acinar plasticity and the downregulation of markers of acinar differentiation in both age groups. Furthermore, we observed upregulation of the senescent marker *Cdkn1a* (Figure A7E). However, the increase was similar in both aging groups, and there were no differences in homeostatic conditions (Table A4). This implies that an increase in the population of senescent cells may not be the cause of the altered stromal response and regenerative capacity associated with aging.

Further examination focused on the differences between age groups in the early response to tissue damage. Differential gene expression analysis identified 1558 differentially expressed genes ($\text{padj} < 0.05$, Table A2), highlighting differences in the response of acinar cells to injury between the old and young mice. Gene set enrichment analysis identified pathways associated with pancreas development, the unfolded protein response, and inflammatory processes enriched in the aged group (Figure 6C). We confirmed the upregulation of transcription factors linked to pancreas development and inflammatory processes, indicating an aggravated response of acinar cells to tissue injury in the aged pancreas. We observed the upregulation of transcription factors promoting an inflammatory response in the pancreas (Figure 6D; Figure A7F). Notably, *Junb* was among the top upregulated genes in the old group. Furthermore, there was an increased expression of *interleukin 33* (*IL-33*), a cytokine involved in promoting the remodeling of the tumor microenvironment and epithelial transformation in preneoplastic lesions, particularly in the presence of *Kras* mutation. Consistent with this finding, KRAS UP signaling pathways were also enriched in old mice. Next, we ask whether *Junb* expression is associated with the difference on gene expression in old mice upon CAE treatment.

Intriguingly, transcriptional analysis of *Junb*-depleted tumors derived from an autochthonous model of pancreatic ductal adenocarcinoma (PDAC) exhibited a significant overlap with the differentially expressed genes in old mice after 5 hours of CAE treatment (Figure 6E). It is important to acknowledge that these comparisons involve different stages of the disease. Nonetheless, our findings revealed a significant overlap in genes differentially expressed between these conditions. These data suggest that *Junb* mediates, at least in part, the transcriptional changes observed in response to injury in old mice. Supporting this observation, the transcription factor binding motif of *Junb* was the most enriched at the promoter regions of differentially expressed genes upon CAE treatment in both age groups (Figure 6F). This indicates a potential connection between the AP-1 targets and the decline in the regenerative capacity of the pancreas observed in old mice. Further exploration of this overlap could provide valuable insights into the mechanisms underlying pancreatic healing and severe acute pancreatitis associated with aging.

Discussion

The process of pancreas recovery following tissue damage requires a coordinated interplay between transcriptional programs of acinar adaptation to injury and various cell types within the regenerative microenvironment. While the impact of aging on tissue repair is well-established across diverse tissues, its precise mechanisms within the pancreas remain largely elusive. Our findings reveal that the pancreas from aged mice lacks the capacity to recover from acute pancreatitis, showing evidence of tissue atrophy and fibroinflammatory stroma. We showed that acinar cells initiate a substantial transcriptional reprogramming even prior to the discernible morphological indicators of tissue remodeling, and even more strongly in aged mice. The exacerbated response of acinar cells to the injury is associated with an increased activation of α SMA + myofibroblasts in old mice, which have been shown to contribute to fibrosis and inflammation.^{26,27} Therefore, our findings show that aging affects the homeostatic mechanism of acinar cells and the stromal remodeling regulating pancreas regeneration.

The reprogramming of acinar cells is crucial to orchestrate the fibroinflammatory response of the pancreas during tissue regeneration.²⁸ Molecular analyses of lesions derived from pancreatitis as well as precursor lesions of cancer, underscore an increasing proinflammatory transcriptional network in the acinar cells associated with disease progression.^{19,29,30} Analysis of chromatin accessibility in sorted acinar cells has identified newly accessible chromatin domains in proinflammatory cytokines during the progression from homeostasis to ADM to KRAS-induced neoplastic

← depicting the overlap between the following datasets. Junb KO: differentially expressed genes in Junb KO vs WT control cell line derived from an autochthonous model of PDAC. Old vs Young: differentially expressed genes in old and young mice at the 5H time point. (F) We analyzed the transcription factor binding sites in the promoter region of differentially expressed genes in old and young mice at the 5H time point by HOMER. The binding site for *Junb* is the top enriched in the set of upregulated genes.

transformation.¹⁷ These studies emphasize the leading role of acinar cells in pancreas regeneration and the implications in disease progression. In our study, we observed an increased number of acinar cells that express the AP-1 family member Junb in old mice. Junb expression in acinar cells during disease progression prevents the resolution of tissue damage and the progression toward precursor lesions of cancer.¹⁶ Mechanistically, JunB co-opts a regulatory network of enhancers activated downstream of KRAS signaling perpetuating an inflammatory environment. Among the secreted factors upregulated in old mice, we observed the cytokine *IL-33*, associated with a fibroinflammatory response, to be exclusively upregulated upon tissue injury in old mice.^{17,31} Notably, transcriptional analysis of sorted acinar cells identifies IL-33 as a mediator of tissue remodeling and promoting disease progression in precursor lesions of PDAC. This indicates that IL-33 may be responsible for the increased number of myofibroblast in old mice after injury. Furthermore, we observed enhanced unfolded protein response in older mice, indicating potential defects in maintaining endoplasmic reticulum homeostasis and a heightened susceptibility to stress in the acinar cells of these mice. Overall, our data suggest that aging exerts changes in the acinar cells that make them prone to a proinflammatory response that is only seen in precursor lesions of PDAC.

Conclusion

Our study reveals that despite the significant differences in the response to injury, the transcriptome of young and old individuals remained remarkably comparable under homeostatic conditions. This suggests that while the transcriptional regulation of acinar function remains robust and resilient to aging processes, acinar cells become sensitized to mounting an inflammatory response following injury. Remarkably, the aged pancreas has notable differences in the methylation patterns of regulatory elements. However, these differences do not necessarily correlate with changes in the transcription of associated genes.³² These insights indicate that variations in the accessibility of regulatory elements could potentially underlie the heightened response to injury associated with aging. In forthcoming experiments, it would be valuable to focus on the cell-autonomous regulatory elements that prime acinar cells toward a proinflammatory response to injury in aged mice.

Recent studies demonstrate the presence of heterogeneous populations of acinar cells characterized by their varying proliferative capacities, possibly contributing to the decline in regenerative potential observed in aged mice. Specifically, aging is associated with the accumulation of metabolically active and cell cycle-arrested senescent cells.³³ While there is increasing evidence of senescent cell buildup in the context of KRAS-induced neoplastic transformation,³⁴ the extent to which senescent cells accumulate with age remains uncertain. Our transcriptome analysis indicated comparable expression levels of senescence markers in young and old mice, with their expression

increasing in response to injury. Interestingly, similar to our findings, skeletal muscles in aged mice harbor a minimal population of senescent cells that increases following injury.³⁵ Collectively, our data suggest that senescent cells in the pancreas are not a direct consequence of the aging process but rather stem from oncogene-induced senescence. Furthermore, our study did not observe alterations in the expression of *telomerase reverse transcriptase (Tert)*, a marker associated with a rare subpopulation of acinar cells possessing regenerative potential.³⁶ We identified a reduction in the expression of markers associated with the Acinar-reg subpopulation, accompanied by an increase in markers characterizing the Acinar-s population in elderly mice. These findings suggest the possibility of clonal amplification among distinct acinar cell populations, each endowed with varying regenerative capacities or susceptibility to damage, which may contribute to the diminished regenerative capability of the pancreas that is observed with aging.

Our study has certain limitations as we used mice that have been housed under sterile conditions with a strictly controlled diet and light/dark cycles. While such conditions are unfeasible to replicate in human subjects, they are indispensable for isolating the effects of aging on pancreas physiology from potential confounding influences of lifestyle-related alterations in transcriptional and cellular composition. Notably, recent functional analyses of genomic variations identified in genome-wide association studies have revealed a connection between the transcriptional dysregulation of the AP-1 complex in acinar cells and an underlying proinflammatory state within the pancreas aggravating the progression of experimental pancreatitis in mice.¹⁴ Thereby underscoring the critical importance of comprehending the impact of aging on the proinflammatory status of acinar cells and the acinar-specific regulatory mechanisms governing the remodeling of the tissue microenvironment and disease progression.

Supplementary Materials

Material associated with this article can be found, in the online version, at <https://doi.org/10.1016/j.gastha.2024.07.002>.

References

1. Baeza-Zapata AA, Garcia-Compean D, Jaquez-Quintana JO, et al. Acute pancreatitis in elderly patients. *Gastroenterology* 2021;161:1736–1740.
2. Quero G, Covino M, Fiorillo C, et al. Acute pancreatitis in elderly patients: a single-center retrospective evaluation of clinical outcomes. *Scand J Gastroenterol* 2019; 54:492–498.
3. Yadav D, Lowenfels AB. The epidemiology of pancreatitis and pancreatic cancer. *Gastroenterology* 2013; 144:1252–1261.
4. Beger HG, Rau BM. Severe acute pancreatitis: clinical course and management. *World J Gastroenterol* 2007; 13:5043–5051.

5. Goodell MA, Rando TA. Stem cells and healthy aging. *Science* 2015;350:1199–1204.
6. Okamura D, Starr ME, Lee EY, et al. Age-dependent vulnerability to experimental acute pancreatitis is associated with increased systemic inflammation and thrombosis. *Aging Cell* 2012;11:760–769.
7. Matsuda Y. Age-related morphological changes in the pancreas and their association with pancreatic carcinogenesis. *Pathol Int* 2019;69:450–462.
8. Jensen JN, Cameron E, Garay MV, et al. Recapitulation of elements of embryonic development in adult mouse pancreatic regeneration. *Gastroenterology* 2005;128:728–741.
9. Pinho AV, Rooman I, Real FX. p53-dependent regulation of growth, epithelial-mesenchymal transition and stemness in normal pancreatic epithelial cells. *Cell Cycle* 2011;10:1312–1321.
10. Brown JW, Cho CJ, Mills JC. Paligenesis: cellular remodeling during tissue repair. *Annu Rev Physiol* 2022;84:461–483.
11. Baer JM, Zuo C, Kang LI, et al. Fibrosis induced by resident macrophages has divergent roles in pancreas inflammatory injury and PDAC. *Nat Immunol* 2023;24:1443–1457.
12. Velez-Delgado A, Donahue KL, Brown KL, et al. Extrinsic KRAS signaling shapes the pancreatic microenvironment through fibroblast reprogramming. *Cell Mol Gastroenterol Hepatol* 2022;13:1673–1699.
13. Carpenter ES, Elhossiny AM, Kadiyala P, et al. Analysis of donor pancreata defines the transcriptomic signature and microenvironment of early neoplastic lesions. *Cancer Discov* 2023;13:1324–1345.
14. Cobo I, Martinelli P, Flandez M, et al. Transcriptional regulation by NR5A2 links differentiation and inflammation in the pancreas. *Nature* 2018;554:533–537.
15. Burdziak C, Alonso-Curbelo D, Walle T, et al. Epigenetic plasticity cooperates with cell-cell interactions to direct pancreatic tumorigenesis. *Science* 2023;380:eadd5327.
16. Li Y, He Y, Peng J, et al. Mutant Kras co-opts a proto-oncogenic enhancer network in inflammation-induced metaplastic progenitor cells to initiate pancreatic cancer. *Nat Cancer* 2021;2:49–65.
17. Alonso-Curbelo D, Ho YJ, Burdziak C, et al. A gene-environment-induced epigenetic program initiates tumorigenesis. *Nature* 2021;590:642–648.
18. Schlesinger Y, Yosefov-Levi O, Kolodkin-Gal D, et al. Single-cell transcriptomes of pancreatic preinvasive lesions and cancer reveal acinar metaplastic cells' heterogeneity. *Nat Commun* 2020;11:4516.
19. Ma Z, Lytle NK, Chen B, et al. Single-cell transcriptomics reveals a conserved metaplasia program in pancreatic injury. *Gastroenterology* 2022;162:604–620.e20.
20. Tosti L, Hang Y, Debnath O, et al. Single-nucleus and in Situ RNA-sequencing reveal cell topographies in the human pancreas. *Gastroenterology* 2021;160:1330–1344.e11.
21. Heinz S, Benner C, Spann N, et al. Simple combinations of lineage-determining transcription factors prime cis-regulatory elements required for macrophage and B cell identities. *Mol Cell* 2010;38:576–589.
22. Keefe MD, Wang H, De La OJ, et al. beta-catenin is selectively required for the expansion and regeneration of mature pancreatic acinar cells in mice. *Dis Model Mech* 2012;5:503–514.
23. Kong B, Bruns P, Behler NA, et al. Dynamic landscape of pancreatic carcinogenesis reveals early molecular networks of malignancy. *Gut* 2018;67:146–156.
24. Pin CL, Rukstalis JM, Johnson C, et al. The bHLH transcription factor *Mist1* is required to maintain exocrine pancreas cell organization and acinar cell identity. *J Cell Biol* 2001;155:519–530.
25. Lopez-Otin C, Blasco MA, Partridge L, et al. Hallmarks of aging: an expanding universe. *Cell* 2023;186:243–278.
26. Ozdemir BC, Pentcheva-Hoang T, Carstens JL, et al. Depletion of carcinoma-associated fibroblasts and fibrosis induces immunosuppression and accelerates pancreas cancer with reduced survival. *Cancer Cell* 2015;28:831–833.
27. Rhim AD, Oberstein PE, Thomas DH, et al. Stromal elements act to restrain, rather than support, pancreatic ductal adenocarcinoma. *Cancer Cell* 2014;25:735–747.
28. Storz P, Crawford HC. Carcinogenesis of pancreatic ductal adenocarcinoma. *Gastroenterology* 2020;158:2072–2081.
29. DelGiorno KE, Chung CY, Vavinskaya V, et al. Tuft cells inhibit pancreatic tumorigenesis in mice by producing prostaglandin D(2). *Gastroenterology* 2020;159:1866–1881.e8.
30. Del Poggetto E, Ho IL, Balestrieri C, et al. Epithelial memory of inflammation limits tissue damage while promoting pancreatic tumorigenesis. *Science* 2021;373:eabj0486.
31. Liew FY, Girard JP, Turnquist HR. Interleukin-33 in health and disease. *Nat Rev Immunol* 2016;16:676–689.
32. Chondronasiou D, Gill D, Mosteiro L, et al. Multi-omic rejuvenation of naturally aged tissues by a single cycle of transient reprogramming. *Aging Cell* 2022;21:e13578.
33. Di Micco R, Krizhanovsky V, Baker D, et al. Cellular senescence in ageing: from mechanisms to therapeutic opportunities. *Nat Rev Mol Cell Biol* 2021;22:75–95.
34. Amor C, Feucht J, Leibold J, et al. Senolytic CAR T cells reverse senescence-associated pathologies. *Nature* 2020;583:127–132.
35. Moiseeva V, Cisneros A, Sica V, et al. Senescence atlas reveals an aged-like inflamed niche that blunts muscle regeneration. *Nature* 2023;613:169–178.
36. Neuhofer P, Roake CM, Kim SJ, et al. Acinar cell clonal expansion in pancreas homeostasis and carcinogenesis. *Nature* 2021;597:715–719.

Received September 22, 2023. Accepted July 3, 2024.

Correspondence:

Address correspondence to: Luis Arnes, PhD, University of Copenhagen, Biotech Research and Innovation Centre, Ole Maaløes Vej 5, Copenhagen 2300, Denmark. e-mail: luis.arnes@bric.ku.dk.

Acknowledgments:

We are sincerely grateful for the Histology and Microscopy, Light Microscopy and Bioinformatics core facilities at the Biotech Research and Innovation Centre (BRIC), University of Copenhagen. Especially, the invaluable support and expertise of Mia Kristine Grønning Høj, Yasuko Antoku and Juliana Assis from the core facilities have significantly contributed to the success of this research. The graphical abstract was created with BioRender.com.

Authors' Contributions:

Acquisition of data: all authors. Drafting of the manuscript: Kristina Høj and Luis Arnes. Critical revision of the manuscript for important intellectual content: all

authors. Obtained funding, Study supervision, Study concept and design: Luis Arnes.

Conflicts of Interest:

The authors disclose no conflicts.

Funding:

Luis Arnes laboratory is supported by core funding of the Biotech Research and Innovation Center, the Danish Cancer Society (R302-A17481, R322-A17.350), The Novo Nordisk Foundation (NNF21OC0070884) and The Innovation Fund (Eurostars 2807). The Novo Nordisk Foundation Center for Stem Cell Biology was supported by Novo Nordisk Foundation grants NNF17CC0027852.

Ethical Statement:

All the animals were treated ethically in accordance with best animal husbandry guideline recommendations of the European Union Directive (2010/63/EU). All the protocols and procedures were approved by the Danish Animal Experiments Inspectorate (2024-15-0201-01673).

Data Transparency Statement:

Study materials will be made available upon request. The transcriptomic and sequencing data discussed in this publication have been deposited in the Gene Expression Omnibus archive (GSE268278).

Reporting Guidelines:

The study was conducted in accordance with ARRIVE guidelines.